Inorg. Chem. **2006**, *45*, 10131–10137

Photosensitizers Containing the 1,8-Naphthyridyl Moiety and Their Use in Dye-Sensitized Solar Cells

Ahmet Kukrek, Dong Wang, Yuanjun Hou, Ruifa Zong, and Randolph Thummel*

Department of Chemistry, 136 Fleming Building, University of Houston, Houston, Texas 77204-5003

Received June 8, 2006

Using a Friedländer condensation approach, we prepared a series of 2-(pyrid-2′-yl)-1,8-naphthyridines containing a carboethoxy group appended at the 4- and 4′-positions. Complexation of these ligands with Ru(II) and NaNCS led to the complexes $[Ru(L)_2(NCS)_2]$, and subsequent hydrolysis of the ester groups afforded the carboxylic acid dyes **13b**–**15b**. The more delocalized and electronegative nature of the 1,8-naphthyridyl moiety lowers the energy of the ligand π^*-level and extends the absorption envelope of these complexes well into the red. The system lacking a 4-carboxypyridine moiety shows poor absorbance in the blue region of the spectrum. Solar cells involving thin films of anatase TiO_2 impregnated with these dyes were prepared, and their photovoltaic performance was evaluated. The incident photon-to-current efficiencies in the region beyond 625 nm were considerably greater than those of the prototype N3 dye.

Introduction

An important aspect of solar energy conversion involves the design and optimization of dye-sensitized solar cells (DSSCs).[1] If properly optimized, DSSCs may function as low cost, efficient alternatives to conventional solid-state semiconductor devices.[2] The main component of a DSSC is a wide band gap semiconductor (>3.0 eV) that is able to accept an electron injected into its conduction band by the excited state of an appropriate photosensitizer. Among a variety of semiconductors, titanium dioxide, in its nanocrystalline (anatase) form, appears to afford superior performance. Anatase TiO_2 is highly mesoporous, providing a large surface area for sensitizer binding and electrolyte access. However, the semiconductor is transparent to the major part of the solar spectrum, and thus, a photosensitizer is required to allow the absorption of light. This sensitizer is the most critical part of the DSSC. Absorption of light by the sensitizer creates a high energy state that can inject the photoexcited electron into the conduction band of TiO_2. Charge injection occurs very rapidly, often requiring less than 1 ps.[3] The injected electron is then swept to the semiconductor bulk by the surface electric field and flows through an external cell to perform useful work. The oxidized dye is subsequently reduced back to the ground state by an electron donor (I^-) present in the electrolyte. Reduction of the oxidized donor (I_3^-) occurs at the counter electrode, and the solar cell is therefore regenerative.

A variety of sensitizers for TiO_2 have been reported, and the most efficient and stable ones are based on ruthenium polypyridyl complexes.[1,2] In particular, *cis*-dithiocyanatobis-

* To whom correspondence should be addressed. E-mail: thummel@uh.edu.

(1) (a) Kalyanasundaram, K.; Grätzel, M. *Coord. Chem. Rev.* **1998**, *77*, 347−414. (b) Nazeeruddin, M. K.; Grätzel, M. *Compr. Coord. Chem. II* **2004**, *9*, 719−758. (c) Grätzel, M. *Inorg. Chem.* **2005**, *44*, 6841−6851. (d) Nazeeruddin, M. K.; Klein, C.; Liska, P.; Grätzel, M. *Coord. Chem. Rev.* **2005**, *249*, 1460−1467.

(2) (a) O'Regan, B.; Grätzel, M. *Nature (London)* **1991**, *353*, 737−740. (b) Nazeeruddin, M. K.; Muller, E.; Humphry-Baker, R.; Vlachopoulos, N.; Grätzel, M. *J. Chem. Soc., Dalton Trans.* **1997**, 4571−4578. (c) Bach, U.; Lupo, D.; Comte, P.; Moser, J. E.; Weissortel, F.; Salbeck, J.; Spreitzer, H.; Grätzel, M. *Nature* **1998**, *395*, 583−585. (d) Hagfeldt, A.; Grätzel, M. *Acc. Chem. Res.* **2000**, *33*, 269−277. (e) Nazeeruddin, M. K.; Pechy, P.; Renouard, T.; Zakeeruddin, S. M.; Humphry-Baker, R.; Comte, P.; Liska, P.; Cevey, L.; Costa, E.; Deacon, G. B.; Bignozzi, C. A.; Grätzel, M. *J. Am. Chem. Soc.* **2001**, *123*, 1613−1624. (f) Renouard, T.; Fallahpour, R. A.; Nazeeruddin, M. K.; Humphry-Baker, R.; Gorelsky, S. I.; Lever, A. B. P.; Grätzel, M. *Inorg. Chem.* **2002**, *41*, 367−378. (g) Klein, C.; Nazeeruddin, M. K.; Di Censo, D.; Liska, P.; Grätzel, M. *Inorg. Chem.* **2004**, *43*, 4216−4226. (h) Klein, C.; Nazeeruddin, M. K.; Liska, P.; Di Censo, D.; Hirata, N.; Palomares, E.; Durrant, J. R.; Grätzel, M. *Inorg. Chem.* **2005**, *44*, 178−180. (i) Schmidt-Mende, L.; Kroeze, J. E.; Durrant, J. R.; Nazeeruddin, M. K.; Grätzel, M. *Nano. Lett.* **2005**, *5*, 1315−1320. (j) Wang, P.; Klein, C.; Humphry-Baker, R.; Nazeeruddin, M. S.; Grätzel, M. *J. Am. Chem. Soc.* **2005**, *127*, 808−809.

(3) (a) Kelly, C. A.; Meyer, J. G. *Coord. Chem. Rev.* **2001**, *211*, 295−315.

10.1021/ic061022a CCC: $33.50
Published on Web 11/10/2006

(4,4′-dicarboxy-2,2′-bipyridine)ruthenium(II) (N3), first pre-

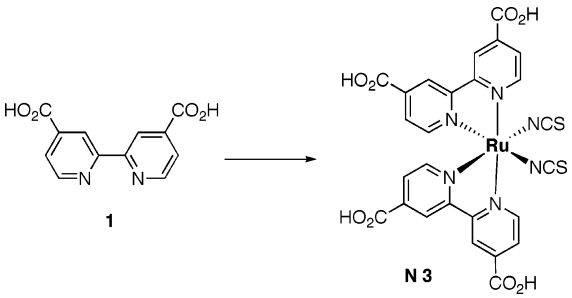

pared by Grätzel and co-workers,[4] has attracted considerable attention. A serious drawback of this sensitizer is the lack of absorption in the near-IR region of the visible spectrum. To further improve the efficiency of DSSCs, the sensitizer should absorb in the near-IR region as well as over the entire visible region of the solar spectrum and be able to maintain sufficient thermodynamic driving force for both the electron injection and the sensitizer regeneration process. The spectral and redox properties of a ruthenium polypyridine complex can be tuned to lower energy by the introduction of a ligand with a lower energy π^*-molecular orbital[5] or a strong donor ligand to destabilize the metal t_{2g} orbital.[6] These conditions are often not compatible for an efficient sensitizer because, in the former case, a too low lying π^*-level would inhibit electron injection into the conduction band of TiO_2, and in the latter case, the easily oxidizable complex cannot be reduced back to the ground state by electron donation from iodide following charge injection into the TiO_2.

Some of the more successful analogues of the N3 dye have involved a variety of perturbations of the polypyridine ligand structure. The position of attachment of the 4,4′-dicarboxy groups has been varied to include the 3,3′- and 5,5′-positions.[7,8] The carboxy anchor groups have been connected to the bipyridine backbone through various linkers.[9] The bipyridine nucleus has been replaced by the closely related 1,10-phenanthroline.[10] To increase the absorption cross-section, a dicarboxy−bpy ligand has been replaced with a bpy having extended conjugation at the 4,4′-positions.[2h] In another effort to increase the absorption envelope of the dye, Arakawa and co-workers lowered the energy of the π^*-excited state of the acceptor ligand by fusing a 5,6-benzo ring to 2,2′-bipyridine (bpy) to create the 2-(pyrid-2′-yl)-quinoline nucleus.[11] Anchoring carboxy groups were introduced at the 4- and 4′-positions to provide ligands **2** and **3**.

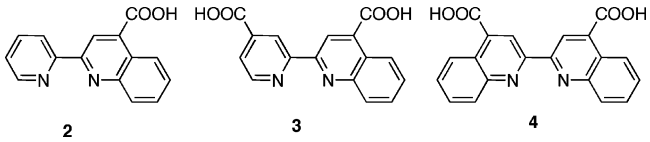

The fusion of two benzo rings afforded the 2,2′-biquinoline ligand **4**.[12] Solar cells made from dyes based on these ligands showed improved absorption properties but somewhat diminished incident photon-to-current efficiencies (IPCEs). Red sensitive ruthenium-based dyes involving terpyridine tricarboxylic acid[1e,13] and phthalocyanine ligands[14] have also been examined.

In earlier work, we have demonstrated that the absorption properties of Ru polypyridine complexes are more influenced by pyrido than benzo fusion.[15] Lower energy absorptions are observed for systems containing ligands that involve 1,8-naphthyrid-2-yl as opposed to quinolin-2-yl. Thus, we decided to prepare and study the ligands **7a**, **12a**,**b**, and their corresponding dye-sensitizer complexes **13**−**15**.

Synthesis and Characterization of the Complexes

The ligand frameworks were assembled through an application of the Friedländer condensation.[16] Thus, 2-amino-nicotinaldehyde (**6**) was treated with methyl 2-acetyliso-

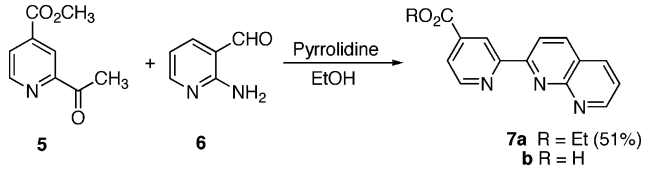

nicotinate (**5**) in the presence of pyrrolidine to afford the ligand **7a**. In ethanol solvent, transesterification to the ethyl ester occurred. In the preparation of ligands **12a**,**b**, the direct incorporation of the carboethoxy groups was not possible. Therefore, these groups were introduced as methyl groups, which could subsequently be oxidized to carboxylic acids and then esterified. Thus, the Friedländer reaction of the 2-acetylpyridines **8a**,**b** with 3-acetyl-2-amino pyridine (**9**) provided **10a**,**b**, which were oxidized with potassium dichromate to the acids **11a**,**b** and finally esterified to **12a**,**b**.

(4) Nazeeruddin, M. K.; Kay, A.; Rodicio, I.; Humphry-Baker, R.; Muller, E.; Liska, P.; Vlachopoulos, N.; Grätzel, M. *J. Am. Chem. Soc.* **1993**, *115*, 6382−6390.
(5) Kalyanasundaram, K.; Grätzel, M.; Nazeeruddin, M. K. *J. Chem. Soc., Dalton Trans.* **1991**, 343−346.
(6) Ruile, S.; Kohle, O.; Pettersson, H.; Grätzel, M. *New J. Chem.* **1998**, 25−31.
(7) Xie, P.-H.; Hou, Y.-J.; Zhang, B.-W.; Cao, Y.; Wu, F.; Tian, W.-J.; Shen, J.-C. *J. Chem. Soc., Dalton Trans*. **1999**, 4217−4221.
(8) Argazzi, R.; Bignozzi, C. A.; Heimer, T. A.; Castellano, F. N.; Meyer, J. G. *Inorg. Chem.* **1994**, *33*, 5741−5749.
(9) (a) Galopponi, E. *Coord. Chem. Rev.* **2004**, *248*, 1283−1297. (b) Yi, H.; Crayston, J. A.; Irvine, J. T. S. *J. Chem. Soc., Dalton Trans.* **2003**, 685−691.
(10) Yanagida, M.; Singh, L. P.; Sayama, K.; Hara, K.; Katoh, R.; Islam, A.; Sugihara, H.; Arakawa, H.; Nazeeruddin, M. K.; Grätzel, M. *J. Chem. Soc., Dalton Trans.* **2000**, 2817−2822.
(11) (a) Yanagida, M.; Yamaguchi, T.; Kurashige, M.; Fujihashi, G.; Hara, K.; Katoh, R.; Sugihara, H.; Arakawa, H. *Inorg. Chim. Acta* **2003**, *351*, 283−290. (b) Yanagida, M.; Yamaguchi, T.; Kurashige, M.; Hara, K.; Katoh, R.; Sugihara, H.; Arakawa, H. *Inorg. Chem.* **2003**, *42*, 7921−7931.
(12) Islam, A.; Sugihara, H.; Singh, L. P.; Hara, K.; Katoh, R.; Nagawa, Y.; Yanagida, M.; Takahashi, Y.; Murata, S.; Arakawa, H. *Inorg. Chim. Acta* **2001**, *322*, 7−16.
(13) Altobello, S.; Argazzi, R.; Caramori, S.; Contado, C.; Da Fré, D.; Rubino, P.; Choné, C.; Larramona, G.; Bignozzi, C. A. *J. Am. Chem. Soc.* **2005**, *127*, 15342−15343.
(14) Nazeeruddin, M. K.; Humphry-Baker, R.; Grätzel, M. *Chem. Commun.* **1998**, 719−720.
(15) Thummel, R. P.; Decloitre, Y. *Inorg. Chim. Acta* **1987**, *128*, 245−249.
(16) (a) Cheng, C.-C.; Yan, S.-J. *Org. React.* **1982**, *28*, 37. (b) Thummel, R. P. *Tetrahedron* **1991**, *47*, 6851−6886.

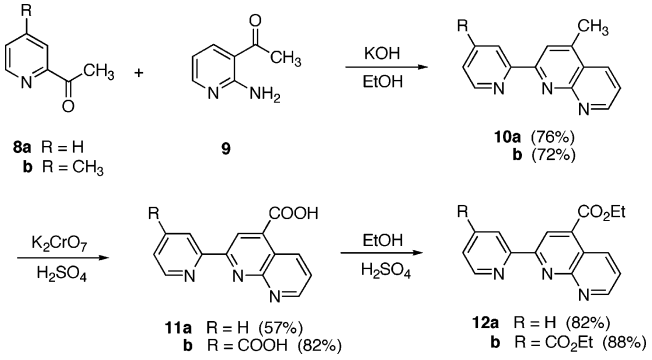

8a R = H
b R = CH_3

9

10a (76%)
b (72%)

11a R = H (57%)
b R = COOH (82%)

12a R = H (82%)
b R = CO_2Et (88%)

Although the dyes require carboxylic acid groups on a ligand to anchor the complex to the semiconductor, the ligands are much easier to isolate, purify, and characterize as their ester derivatives. The ester was therefore treated with 0.5 equiv of an appropriate Ru(II) source followed by sodium thiocyanate to afford complexes **13a**−**15a**, which were

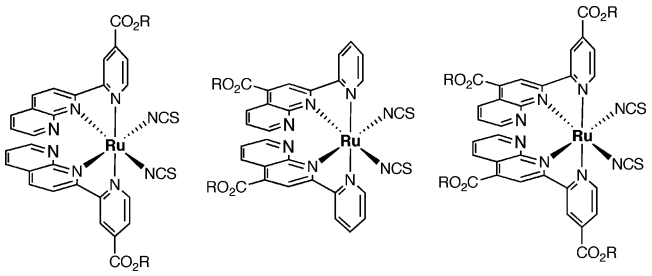

13a R = Et
b R = H

14a R = Et
b R = H

15a R = Et
b R = H

purified by chromatography and characterized by ^{1}H NMR, IR, and CHN analysis. The final carboxylic acid substituted dyes were prepared by hydrolysis of the ester groups.

Because the pyridylnaphthyridine (pynap) ligands are unsymmetrical about the 2,2′-bond, three diastereomeric complexes $[RuL_2(NCS)_2]$ are possible in which the two thiocyanate ligands remain cis to one another. A trans disposition of the two thiocyanates is unlikely because of severe interligand steric interactions between the pynaps. The diastereomer in which a pyridine from one ligand is trans to the naphthyridine from the other ligand can be eliminated because this would require both ligands to be nonequivalent, affording unique ^{1}H signals for all the aromatic protons. The two more symmetrical diastereomers would either have the two pyridines located trans to one another or the two naphthyridines located trans to one another.

Using a combination of chemical shift, multiplicity, and 2D-connectivity information from the ^{1}H NMR spectra, complete proton assignments for the ligands **7a**, **12a**,**b**, and complexes **13a**−**15a** have been made and are summarized in Table 1. At 300 MHz, the signals were well-resolved and the correlation was straightforward. This NMR data are consistent with the diastereomer having the pyridines located trans to one another as depicted in structures **13**−**15**. The characteristic proton signals are H7 on naphthyridine and H6′ on pyridine. In the free ligand, H7 appears at low field (9.15−9.22 ppm), being deshielded by the adjacent nitrogen. In the complex, however, H7 is held over the shielding region of the pyridine ring of the orthogonal ligand and is thus shifted to higher field by 1.12−1.34 ppm.[17] In contrast, H6′ appears at somewhat higher field than H7 in the free ligand. In the complex, however, it is held close to the deshielding region of the orthogonal thiocyanate ligand and is thus shifted to lower field by 0.50−0.83 ppm. These shielding and deshielding effects are consistent with what is observed for H6 and H6′ of the N3 dye.[18] In the following discussion, we shall find that the stereochemical disposition of the ligands may indeed play an important role in determining the photophysical properties of the dyes.

Table 1. ^{1}H NMR Chemical Shift Data[a] for the Ligands and Complexes[b,c]

ligand or complex	H3	H4	H5	H6	H7	H3′	H4′	H5′	H6′
7a	8.69	8.65	8.55	7.69	9.15	9.07		7.99	8.98
13a	8.51	8.99	8.38	7.44	8.03	9.32		8.30	9.61
					(+1.12)				(−0.63)
12a	9.09		9.14	7.78	9.21	8.82	7.61	8.09	8.65
14a	9.00		8.91	7.50	7.96	9.30	7.91	8.32	9.15
					(+1.25)				(−0.50)
12b	9.37		9.30	7.63	9.22	9.26		8.00	8.92
15a	9.07		9.16	7.30	7.88	8.79		8.14	9.75
					(+1.34)				(−0.83)

[a] Recorded at room temperature in DMSO-d_6 except **12b** and **15a**, which were recorded in $CDCl_3$. [b] The prime notation indicates protons of the pyridine ring. The coordination-induced shift in ppm is given in parentheses. [c] The ethyl ester signals appeared as a 2H quartet at 4.45−4.60 ppm and a 3H triplet at 1.40−1.55 ppm.

The IR spectra of complexes **13a**−**15a**, measured as a solid sample, show a strong, intense NCS stretching band in the region 2098−2107 cm^{-1}, which is consistent with N-coordination of this ligand.[19] The bands in the region 1704−1720 cm^{-1} are assigned to the C═O stretching mode of the carboxy groups.

Photophysical and Electrochemical Behavior

The electronic absorption spectra of the dye complexes as their ethyl ester derivatives were measured in CH_2Cl_2, and the data are summarized in Table 2 along with similar data for the dyes as the free carboxylic acids measured in MeOH. Strong $\pi-\pi^*$ absorptions for the coordinated ligands are observed in the region of 326−346 nm. At lower energy, the metal-to-ligand charge transfer (MLCT) absorption is observed as two partially resolved bands (Figures 1 and 2). The longer wavelength band shows some vibrational structure, which is consistent throughout the series **13**−**15**.

Several features of these spectra are noteworthy. First, the absorption envelope for the ester dyes **14a** and **15a**, containing a 4-carboethoxynaphthyridyl moiety, extends far into the low energy region of the spectrum, reaching to the near-IR (900 nm). In contrast, the system involving the unsubstituted naphthyridyl moiety, **13a**, is a poorer excited-state charge acceptor and thus shows a smaller absorption envelope in

(17) (a) Zabri, H.; Gillaizeau, I.; Bignozzi, C. A.; Caramori, S.; Charlot, M. F.; Cano-Boquera, J.; Odobel, F. *Inorg. Chem.* **2003**, *42*, 6655−6666. (b) Thummel, R. P.; Lefoulon, F. *Inorg. Chem.* **1987**, *26*, 675−680.
(18) Shklover, V.; Nazeeruddin, M. K.; Zakeeruddin, S. M.; Barbé, C.; Kay, A.; Haibach, T.; Steurer, W.; Hermann, R.; Nissen, H. U.; Grätzel, M. *Chem. Mater.* **1997**, *9*, 430−439.
(19) Kohle, O.; Ruile, S.; Grätzel, M. *Inorg. Chem.* **1996**, *35*, 4779−4787.

Table 2. Electronic Absorption Maxima of **13**−**15** as Their Esters and Free Acids[a]

complex	λ_{max}, nm (δ)
13a	233 (38 440), 244 (37 280), 273 (20 530), 338 (40 470), 420 (9080), 543 (5210), 613 (7830), 760 (2240)
14a	233 (38 460), 245 (38 980), 268 (28 520), 335 (40 010), 460 (2330), 579 (8850), 655 (10 130), 810 (5180)
15a	233 (44 150), 247 (42 290), 279 (23 720), 346 (44 680), 425 (10 990), 573 (7650), 648 (10 440), 797 (4700)
13b	256 (26 670), 333 (38 970), 388 (8360), 532 (6500), 579 (7400)
14b	211 (48 540), 238 (33 710), 263 (23 660), 326 (31 700), 537 (6220), 593 (7030)
15b	211 (45 780), 244 (31 430), 274 (15 710), 336 (30 740), 405 (5950), 538 (4860), 599 (6330)

[a] Esters (**13a**−**15a**) recorded in 5×10^{-5} M CH_2Cl_2, acids (**13b**−**15b**) recorded in 5×10^{-5} M MeOH. (For **13b**, 9% DMF was used to increase solubility.)

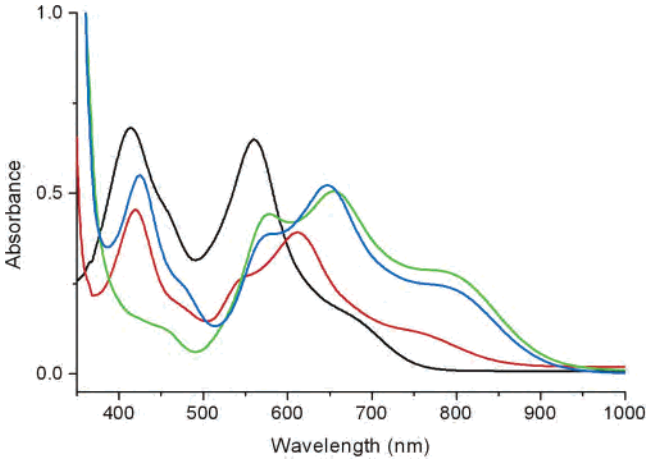

Figure 1. Electronic absorption spectra of the dyes as their ethyl esters, 5×10^{-5} M in CH_2Cl_2: **13a** (red), **14a** (green), **15a** (blue), along with N3 dye (black).

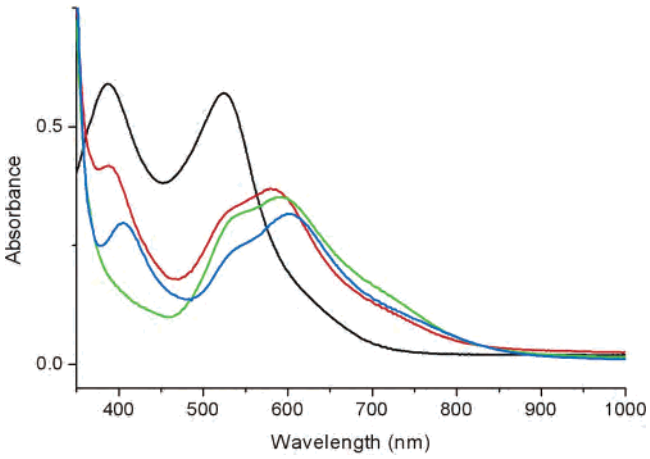

Figure 2. Electronic absorption spectra of the dyes as their free carboxylic acids, 5×10^{-5} M in MeOH (**13b** contains 9% DMF to improve solubility): **13b** (red), **14b** (green), **15b** (blue), and N3 dye (black).

this low energy region (Figure 1). For the higher energy MLCT bands, the situation is somewhat different. A strong absorbance at 420 and 425 nm is observed for **13a** and **15a**, respectively, and this band correlates well with a similar band for the ethyl ester of the N3 dye. All three of these systems possess two 4-carboethoxypyridine moieties located trans to one another. The absorbance at about 420 nm is essentially absent for the **14a** complex, which lacks a carboethoxy substituent on the two pyridine rings.

Table 3. Emission, Electrochemical, and IPCE Properties of the Dyes **13b**−**15b**

dyes	emission[a] λ_{max}, nm	emission[a] E^{0-0}, eV	$E_{1/2}$(ox)[b] (δE)	$E_{1/2}$(red)[b,c] (δE)	E^*(ox), V	IPCE max, %
13b	743	1.91	0.75 (100)	−1.12 (10), −1.37 (25)	−1.16	71
14b	750	1.91	0.83 (76)	−0.89 (51), −1.11 (89)	−1.08	43
15b	750	1.87	0.82 (147)	−0.76 (96), −0.97 (83)	−1.05	58

[a] Obtained at room temperature in a degassed 10^{-5} M methanol solution by exciting at the lowest energy MLCT band. [b] Measured with a glassy carbon electrode at 100 mV/s in DMF containing 0.1 M N(*n*-Bu)$_4$PF$_6$ and reported in volts relative to SCE; the difference between the anodic and cathodic waves is given in parentheses (mV). [c] Reductions of the acids were not clear; data are presented for the corresponding esters **13a**−**15a**.

When the ester dyes are converted to acids, the absorption maxima shift to higher energy and the low energy absorption envelopes for **13a**−**15a** now all appear to be quite similar with maxima at 579−599 nm (Figure 2). This envelope reaches well into the red, dropping to zero only at about 850 nm. For the region around 400 nm, an absorption for **14b** is again conspicuously missing, pointing once more to the importance of the 4-carboxypyridine motif. This same behavior is evidenced for the dyes derived from the two pyridylquinoline ligands, **2** and **3**, examined earlier by Arakawa and co-workers. Although two MLCT bands are observed for [Ru(**3**)$_2$(NCS)$_2$], the higher energy band is missing for [Ru(**2**)$_2$(NCS)$_2$], which does not contain a 4-carboxy substituted pyridine.[11a] The 4-carboethoxy substituent increases the electron accepting ability of the pyridine ligand and thus explains the appearance of this higher energy component of the MLCT transition at about 400 nm. This geometric feature may be a key to effective dye design and emphasizes the critical importance of the stereochemical arrangement of such complexes.

When excited at their MLCT maxima, all three dye complexes show weak emissions. The emission energies for **14b** and **15b** are the same, but complex **13b**, which lacks the 4-carboxynaphthyridyl group, emits at higher energy, 743 nm. From a tangent to the high energy side of the room-temperature emission spectrum, one can estimate the energy of the 0−0 band,[20] and this value (in eV) is listed in Table 3.

The half-wave potentials for the three dyes were determined by cyclic voltammetry in DMF, and the data are presented in Table 3. Each complex shows one metal-based oxidation and two ligand-based reduction couples. It appears that a carboxy group on the naphthyridine ring, as in **14b** and **15b**, has a more important effect on the oxidation potential, causing an increase of 70−80 mV relative to that of **13b**.

The oxidation potential of a sensitizer in the excited state (E^*_{ox}) has an important influence on the electron-transfer process. To get efficient injection of an electron into the conduction band of TiO_2, this potential should be more

(20) Caspar, V. J.; Westmoreland, D.; Allen, G. H.; Bradley, P. G.; Meyer, T. J.; Woodruff, W. H. *J. Am. Chem. Soc.* **1984**, *106*, 3492−3500.

Figure 3. Thin film of anatase TiO_2 coated on FTO glass impregnated with dye **13b** (left), **14b** (middle), and **15b** (right).

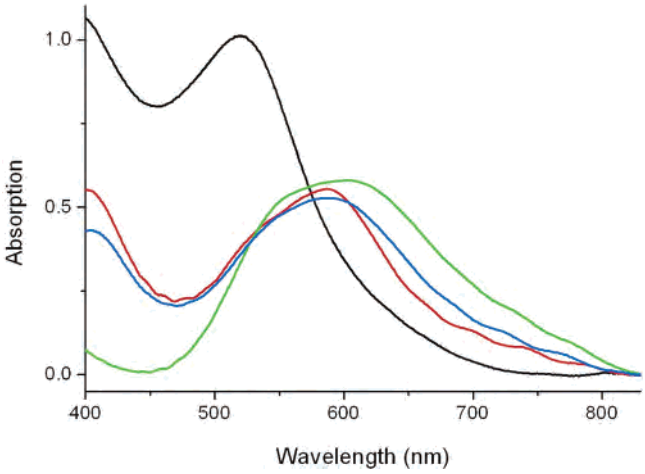

Figure 4. Electronic absorption spectra of the dye impregnated films of TiO_2 coated on FTO glass: **13b** (red), **14b** (green), **15b** (blue), and N3 dye (black).

negative than the band edge of −0.80 V.[11b,12] The excited-state oxidation potential can be estimated from[20]

$$E^*_{ox} = E_{1/2}(ox) - E^{0-0} \quad (1)$$

where E^{0-0} is the minimum energy difference between the ground and excited states as estimated by a tangent to the high energy side of the emission spectrum at room temperature. Furthermore, the ground-state oxidation potentials ($E_{1/2}$(ox)) of **13b**−**15b** are sufficiently positive to be reduced by iodide ($E_{1/2}(I^-/I_3^-) = +0.2$ V).

Photovoltaic Performance

The photovoltaic performance of thin films of anatase TiO_2 impregnated with the dyes **13b**−**15b** was evaluated using an electrolyte solution of I^-/I_3^- in acetonitrile as the electron mediator. Transparent films of anatase TiO_2 on FTO glass slides were prepared in the normal manner[21] and immersed in a methanol−DMSO (10:1) solution of the dye for 14 h. The impregnated films are illustrated in Figure 3, and the absorption spectra of the films containing the three dyes are shown in Figure 4 along with a film containing the N3 dye. A solar cell was constructed from these thin films and

(21) Barbe, Ch. J.; Arendse, F.; Comte, P.; Jirousek, M.; Lenzmann, F.; Shklover, V.; Grätzel, M. *J. Am. Ceram. Soc.* **1997**, *80*, 3157−3171.

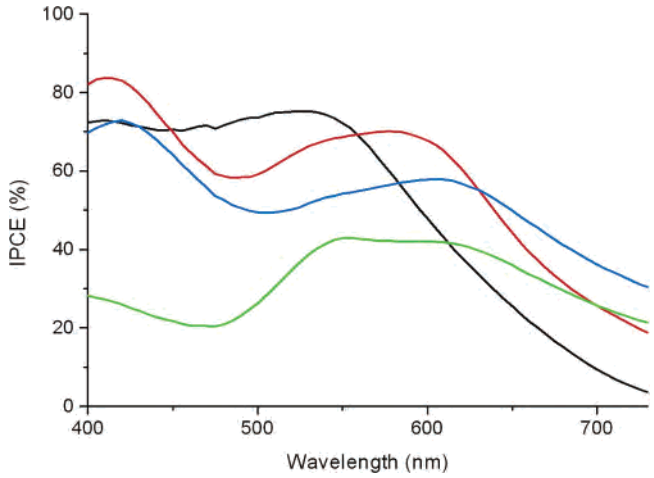

Figure 5. Photoaction spectra obtained for TiO_2 films impregnated with sensitizer dyes: **13b** (red), **14b** (green), **15b** (blue), and N3 (black).

irradiated over the region from 400 to 750 nm. The photocurrent action spectra were obtained in this manner and are shown in Figure 5 along with a spectrum of a film similarly impregnated with the N3 dye measured at the same time for comparison purposes.

The photocurrent action spectra show several important features. First, the band shapes closely parallel the absorption spectra for the dyes, as shown in Figure 2. For **13b** and **15b**, there is a maximum at about 415 nm, which is lacking for **14b**. The low energy portion of the curves extends into the near-infrared and the IPCEs for the three pynap dyes at 700 nm vary from 25 to 36%, which is considerably greater than the 10% observed for N3. The dyes **13b** and **15b** clearly perform better than **14b**, and the integrated area under the curves for these two species (100 for **13b** and 93 for **15b**) considerably exceed N3 (88). These values become even more disparate if one considers only the region from 575 to 725 nm. With regard to peak IPCE performance, N3 shows the top efficiency at 75%, **13b** is not far behind at 71%, and **15b** is respectable at 58%. Because of the lower lying π^*-orbitals of the 1,8-naphthyridine directly coordinated to Ru, IPCE behavior in the red region for dyes containing this moiety is markedly superior.

The behavior of the three pynap dye sensitizers roughly tracks their estimated excited-state oxidation potentials, as listed in Table 3. With the most negative E^*(ox) of −1.16 V, **13b** is the more effective dye; **14b** and **15b**, with more positive values of E^*(ox), are less effective. Although it is difficult to draw any strong conclusions from looking at only three closely related systems, it appears that the incorporation of a 1,8-naphthyridyl moiety can extend the dye performance further into the red region of the spectrum and the existence of a 4-carboxypyridine moiety is an important feature for maintaining optimal higher energy performance. Thus the dye **14b**, which lacks a 4-carboxy substituent, behaves the least effectively. Electronegativity and delocalization effects in polypyridyl-type ligands can influence sensitizer dye efficiencies in a predictable manner. Future studies will examine how other strategic variations in ligand design can be used to further optimize solar cell performance.

Experimental Section

NMR spectra were obtained on a General Electric QE−300 spectrometer at 300 MHz for ^{1}H and 75 MHz for ^{13}C, referenced to TMS, DMSO-d_6, and CD_3CN. IR spectra were measured on a Thermo Nicolet AVATAR 370 Fourier transform (FT) IR spectrophotometer. UV−vis spectra were recorded on a Perkin-Elmer Lambda 3B or a Hewlett-Packard 8453 spectrophotometer. All spectra were corrected for the background spectrum of the solvent. Emission spectra were obtained on a Perkin-Elmer LS50B luminescence spectrometer after degassing the sample with a stream of Ar. Electrochemical measurements were carried out using a BAS Epsilon electroanalytical system. Cyclic voltammetry (CV) experiments were performed at room temperature in a one-compartment cell equipped with a glassy carbon working electrode, a saturated calomel reference electrode (SCE), and a platinum wire as the auxiliary electrode in acetonitrile or DMF containing 0.1 M tetrabutylammonium hexafluorophosphate at a scan rate of 100 mV s^{-1}. Both solvents were distilled from CaH_2. Melting points were measured with a Thomas-Hoover capillary melting-point apparatus and are uncorrected. Elemental analyses were carried out by QTI, P.O. Box 470, Whitehouse, NJ 08888-0470. 2-Aminonicotinaldehyde (**6**),[22] 3-acetyl-2-aminopyridine (**9**),[23] and the N3 dye[18] were prepared according to published procedures. All solvents were reagent grade.

Solar Cell Preparation and IPCE Measurements. The acidic TiO_2 colloid was prepared following a published procedure.[21] This TiO_2 paste was then coated onto a conducting SnO_2:F-coated (FTO) glass slide (16 × 45 mm) using a glass rod spreader and adhesive tape as a spacer. The TiO_2 films were heated at 130 °C for 5 min and 450 °C for 30 min in air, resulting in a transparent film. After cooling to 80 °C, the slide was immediately dipped into a small vial containing 10 mL of a 1.0 mmol solution of the dye in 10:1 MeOH/DMSO. The slide was soaked for 14 h and then washed with MeOH and dried in air.

The photoaction spectrum is obtained from a dye-sensitized solar cell arranged as a two-electrode sandwich.[8] The dye-impregnated TiO_2 film on FTO conducting glass acts as the photoanode. The counter electrode consists of a thin film of platinum sputtered on FTO glass. The redox mediator is 0.5 M LiI/0.05 M I_2 in acetonitrile. The cell is assembled by clamping together the TiO_2 photoanode and the counter electrode with a specially designed Teflon cell holder (Supporting Information, Figure SI-1) in between. The holder has a round aperture with an area of 0.21 cm^2 to admit light. The redox mediator is introduced into the aperture by slow addition of the electrolyte solution through a hole at the top of the cell holder. The photoanode is oriented toward the light source, and the cell is illuminated with a 75 W Xe lamp coupled to a Cornerstone 260 monochromator. Photocurrents are measured under short circuit conditions with a Keithly model 2000 digital electrometer. Incident irradiance is measured with a calibrated UDT model 260 silicon photodiode (aperture area = 0.44 cm^2).

Methyl 2-Acetylisonicotinate (5). A mixture of methylisonicotinate (1.37 g, 10 mmol), pyruvic acid (2.64 g, 30 mmol), $AgNO_3$ (0.136 g, 0.8 mmol), $(NH_4)_2S_2O_8$ (3.42 g, 15 mmol), and CF_3COOH (1.14 g, 10 mmol) in H_2O/ CH_2Cl_2 (3:7, 100 mL) was stirred for 2 h at 40 °C. The solution was made basic by adding NaOH pellets. The organic phase was separated, and the aqueous residue was extracted with CH_2Cl_2 (3 × 10 mL). After evaporation of the CH_2Cl_2, the residue was chromatographed on silica gel, eluting with hexane/CH_2Cl_2/EtOAc (4:1:1), to provide **5** as a beige solid (0.91 g, 50%), mp 49−51 °C: ^{1}H NMR ($CDCl_3$, δ) 8.82 (d, 1H), 8.54 (s, 1H), 8.01 (dd, 1H), 3.96 (s, 3H), 2.74 (s, 3H); ^{13}C NMR ($CDCl_3$, δ) 199.4, 165.2, 154.6, 150.0, 138.7, 126.2, 121.1, 53.1, 26.1.

2-(4′-Carboethoxypyrid-2′-yl)-1,8-naphthyridine (7a). A mixture of methyl 2-acetylisonicotinate (**5**, 0.24 g, 1.34 mmol), 2-aminonicotinaldehyde (**6**, 0.16 g, 1.34 mmol), and pyrrolidine (0.1 g, 1.47 mmol) in ethanol (8 mL) was heated at reflux for 48 h. After evaporation of the solvent, the residue was chromatographed on alumina, eluting with CH_2Cl_2/EtOAc (3:1), to provide **7a** as a yellow solid (0.19 g, 51%), mp 104−5 °C: ^{13}C NMR ($CDCl_3$, δ) 165.3, 158.8, 156.7, 155.9, 154.1, 149.9, 139.3, 138.1, 137.2, 124.0, 123.2, 122.7, 122.5, 121.8, 120.3, 62.0, 14.5. Anal. Calcd for $C_{16}H_{13}N_3O_2$: C, 68.8; H, 4.69; N, 15.04. Found: C, 68.34; H, 4.48; N, 14.81.

4-Methyl-2-(pyrid-2′-yl)-1,8-naphthyridine (10a). A mixture of 2-acetylpyridine (**8a**, 0.19 g, 1.65 mmol), 3-acetyl-2-aminopyridine (**9**, 0.13 g, 0.98 mmol), and KOH (0.15 mL, 0.9 M) in ethanol (10 mL) was heated at reflux for 48 h. After evaporation of the solvent, the residue was chromatographed on alumina, eluting with CH_2Cl_2/EtOAc (3:1), to provide **10a** as a light brown solid (0.16 g, 76%), mp 82−3 °C: ^{1}H NMR ($CDCl_3$, δ) 9.11 (dd, 1H), 8.85 (d, 1H), 8.71 (d, 1H), 8.55 (s, 1H), 8.38 (dd, 1H), 7.87 (ddd, 1H), 7.48 (dd, 1H), 7.36 (dd, 1H), 2.78 (s, 3H, CH_3); ^{13}C NMR ($CDCl_3$, δ) 158.9, 155.8, 153.5, 149.1, 146.7, 139.9, 137.2, 133.4, 124.7, 123.1, 122.7, 121.8, 120.5, 18.5.

4-Carboxy-2-(pyrid-2′-yl)-1,8-naphthyridine (11a). To a solution of **10a** (0.15 g, 0.68 mmol) in concentrated H_2SO_4 (5 mL) in an ice bath was added $K_2Cr_2O_7$ (0.45 g, 1.5 mmol) in small portions over a period of 1 h. After addition of dichromate, stirring at room temperature was continued overnight. The deep green reaction mixture was then poured into ice−water (100 mL) and adjusted to pH 4−5 with solid Na_2CO_3. The white precipitate was collected, washed with water, and air-dried to provide **11a** as a pink solid (97 mg, 57%), mp >250 °C: ^{1}H NMR (DMSO-d_6, δ) 9.21 (dd, 2H), 9.01 (s, 1H), 8.81 (d, 1H), 8.64 (d, 1H), 8.08 (t, 1H), 7.76 (dd, 1H), 7.6 (dd, 1H).

4-Carboethoxy-2-(pyrid-2′-yl)-1,8-naphthyridine (12a). A mixture **11a** (75 mg, 0.29 mmol) and ethanol (5 mL) containing concentrated H_2SO_4 (0.1 mL) was heated at reflux for 24 h. The reaction mixture was cooled, poured into water (10 mL), and adjusted to pH 8 with solid K_2CO_3. The mixture was then extracted with $CHCl_3$ (3 × 10 mL) and the combined organic layers were dried over $MgSO_4$. After evaporation of the solvent, **12a** was obtained as a pink solid (68 mg, 82%), mp 118−9 °C: ^{13}C NMR ($CDCl_3$, δ) 165.5, 159.1, 156.3, 154.8, 154.1, 149.3, 137.3, 137.1, 135.6, 125.2, 123.3, 122.7, 121.5, 120.7, 62.3, 14.5. Anal. Calcd for $C_{16}H_{13}N_3O_2 \cdot 0.25\ H_2O$: C, 67.72; H, 4.76; N, 14.81. Found: C, 67.59; H, 4.55; N, 14.55.

4-Methyl-2-(4′-methylpyrid-2′-yl)-1,8-naphthyridine (10b). Treatment of 2-acetyl-4-methylpyridine (**8b**, 0.25 g, 1.82 mmol), 3-acetyl-2-aminopyridine (**9**, 0.24 g, 1.82 mmol), and KOH (0.54 mL, 0.9 M) in the manner described above for **10a** provided crude material, which was chromatographed on alumina, eluting with CH_2Cl_2/EtOAc (6:1), to give **10b** as a white solid (0.3 g, 72%), mp 102−3 °C: ^{1}H NMR ($CDCl_3$, δ) 9.13 (dd, 1H), 8.75 (d, 1H), 8.59 (m, 2H), 8.41 (dd, 1H), 7.51 (dd, 1H), 7.23 (d, 1H), 2.80 (s, 3H, CH_3), 2.48 (s, 3H, CH_3).

4-Carboethoxy-2-(4′-carboethoxypyrid-2′-yl)-1,8-naphthyridine (12b). Following the procedure for **11a**, $K_2Cr_2O_7$ (1.68 g, 5.7 mmol) was added in small portions over 1 h to an ice-cold solution of **10b** (0.3 g, 1.3 mmol) in concentrated H_2SO_4 (10 mL) to provide **11b** as a pink solid (0.32 g, 82%), mp: >250 °C. Due to poor

(22) Majewicz, T. G.; Caluwe, P. *J. Org. Chem.* **1974**, *39*, 720−721.
(23) Murray, J. M.; Zimmerman, S. C.; Kolotuchin, S. V. *Tetrahedron* **1995**, *51*, 635−648.

solubility, **11b** was not further characterized but used directly in the next step. Following the procedure for **12a**, the reaction of **11b** (0.31 g, 1.04 mmol) with concentrated H_2SO_4 in ethanol provided **12b** as a light-brown solid (0.32 g, 88%), mp 166−9 °C: ^{13}C NMR ($CDCl_3$, δ) 165.4,165.2, 158.5, 156.3, 155.9, 154.2, 150, 139.4, 137.2, 135.6, 124.4, 123.5, 121.7, 121.6, 120.9, 62.3, 62.1, 14.5, 14.4. Anal. Calcd for $C_{19}H_{17}N_3O_4 \cdot 0.25\ H_2O$: C, 64.13; H, 4.92; N, 11.81. Found: C, 63.99; H, 4.82; N, 11.5.

***cis*-[Ru(7a)$_2$(NCS)$_2$] (13a).** A mixture of $RuCl_3 \cdot 3H_2O$ (50 mg, 0.19 mmol) and **7a** (100 mg, 0.38 mmol) in ethanol (15 mL) was refluxed for 72 h. To this reaction mixture was added a solution of NaNCS (0.25 g, 3.05 mmol) in water (5 mL), and reflux was continued overnight under reduced light. After evaporation of the solvent, the dark residue was washed with water and chromatographed on alumina, eluting with CH_2Cl_2/EtOAc (5:1). A green band was collected to give *cis*-[Ru(**7a**)$_2$(NCS)$_2$] as a black solid (36 mg, 27%): IR 2104 cm^{-1} (NCS). Anal. Calcd for $C_{34}H_{26}N_8O_4RuS_2 \cdot H_2O$: C, 51.44; H, 3.55; N, 14.11. Found: C, 51.12; H, 3.32; N, 13.84.

***cis*-[Ru(12a)$_2$(NCS)$_2$] (14a).** A mixture of [Ru(DMSO)$_4$Cl$_2$] (87 mg, 0.17 mmol) and **12a** (100 mg, 0.35 mmol) in $CHCl_3$ (15 mL) was heated at reflux overnight. After evaporation of $CHCl_3$, ethanol (20 mL) and a solution of NaNCS (0.23 g, 2.84 mmol) in water (7 mL) were added and reflux was continued for 72 h under reduced light. After evaporation of the solvent, the dark residue was washed with water and chromatographed on alumina, eluting with CH_2Cl_2/EtOAc (5:1). A green band was collected, which provided *cis*-[Ru(**12a**)$_2$(NCS)$_2$] as a dark blue solid (74 mg, 54%): IR 2104 cm^{-1} (NCS). Anal. Calcd for $C_{34}H_{26}N_8O_4RuS_2 \cdot H_2O$: C, 51.44; H, 3.55; N, 14.11. Found: C, 51.02; H, 3.30; N, 13.74.

***cis*-[Ru(12b)$_2$(NCS)$_2$] (15a).** Treatment of [Ru(DMSO)$_4$Cl$_2$] (67 mg, 0.13 mmol) and **12b** (100 mg, 0.28 mmol) in the manner described above for **14a** provided material that was chromatographed on alumina, eluting with CH_2Cl_2, to provide *cis*-[Ru(**12b**)$_2$(NCS)$_2$] as a deep green solid (44 mg, 35%): IR 2100 cm^{-1} (NCS). Anal. Calcd for $C_{40}H_{34}N_8O_8RuS_2 \cdot EtOH$: C, 52.22; H, 4.17; N, 11.59. Found: C, 52.12; H, 3.95; N, 11.05.

***cis*-[Ru(7b)$_2$(NCS)$_2$] (13b).** To a solution of *cis*-[Ru(**7a**)$_2$(NCS)$_2$] (16 mg, 0.020 mmol) in THF (4 mL) was added a 40% aqueous solution of NBu_4OH (0.25 mL), and the mixture was stirred for 30 min at room temperature. The solution was diluted with water (7.5 mL), concentrated under vacuum, and adjusted to pH 3 with CH_3CO_2H. A blue precipitate was collected, washed with water, and air-dried to provide *cis*-[Ru(**7b**)$_2$(NCS)$_2$] (13 mg, 76%): ^{1}H NMR (DMSO-d_6, δ) 9.57 (d, J = 6.0 Hz, 2H), 9.29 (s, 2H), 8.95 (d, J = 8.1 Hz, 2H), 8.47 (d, J = 8.4 Hz, 2H), 8.37 (d, J = 8.1 Hz, 2H), 8.25 (d, J = 5.4 Hz, 2H), 8.00 (d, J = 3.0 Hz, 2H) 7.42 (dd, J = 3.6, 7.8 Hz, 2H); IR 2107 cm^{-1} (NCS). Anal. Calcd for $C_{30}H_{17.5}N_8O_4RuS_2 \cdot 0.5(n\text{-}Bu)_4N \cdot H_2O$: C, 53.17; H, 4.40; N, 13.87. Found: C, 52.99; H, 4.18; N, 12.85.

***cis*-[Ru(11a)$_2$(NCS)$_2$] (14b).** Treatment of *cis*-[Ru(**12a**)$_2$(NCS)$_2$] (15 mg, 0.019 mmol) in the manner described above for **13b** provided a blue solid. The material was dissolved in a minimum amount of methanol, diluted with water, and adjusted to pH 3 with CH_3CO_2H to give a precipitate. This procedure was repeated two more times to afford *cis*-[Ru(**11a**)$_2$(NCS)$_2$] as a blue solid (9 mg, 58%): ^{1}H NMR (DMSO-d_6, δ) 9.31 (d, J = 5.4 Hz, 2H), 9.14 (d, J = 5.1 Hz, 2H), 8.99 (br, 4H), 8.28 (t, J = 8.1 Hz, 2H), 7.96 (d, J = 3.0 Hz, 2H), 7.90 (t, J = 6.6 Hz, 2H), 7.47 (dd, J = 4.5, 8.1 Hz, 2H); IR 2098 cm^{-1} (NCS). Anal. Calcd for $C_{30}H_{18}N_8O_4RuS_2 \cdot CH_3CO_2H \cdot 3H_2O$: C, 47.11; H, 3.21; N, 13.74. Found: C, 46.59; H, 2.97; N, 13.28.

***cis*-[Ru(11b)$_2$(NCS)$_2$] (15b).** Treatment of *cis*-[Ru(**12b**)$_2$(NCS)$_2$] (19 mg, 0.020 mmol) in the manner described above for **14b** provided *cis*-[Ru(**11b**)$_2$(NCS)$_2$] as a green solid (9 mg, 48%): ^{1}H NMR (DMSO-d_6, δ) 9.52 (d, J = 5.4 Hz, 2H), 9.37 (s, 2H), 9.11 (s, 2H), 8.96 (br, 2H), 8.30 (d, J = 6.9 Hz, 2H), 8.01 (d, J = 2.7 Hz, 2H), 7.49 (br, 2H); IR 2102 cm^{-1} (NCS). Anal. Calcd for $C_{32}H_{18}N_8O_8RuS_2 \cdot CH_3CO_2H \cdot 2H_2O$: C, 45.18; H, 2.90; N, 12.40. Found: C, 45.06; H, 2.67; N, 12.26.

Acknowledgment. We thank the Robert A. Welch Foundation (E-621) and the National Science Foundation (CHE-0352617) for financial support of this work. We also thank Professor Gerald Meyer and Dr. Andras Marton for patient advice and guidance in solar cell preparation and evaluation.

Supporting Information Available: Diagram of Teflon cell for solar cell measurements and ^{1}H NMR spectra of **13b**, **14b**, and **15b**. The material is available free of charge via the Internet at http://pubs.acs.org.

IC061022A